Cylinder-to-Cylinder Variations in Diesel Dual Fuel Combustion under Low-load Conditions

Orawan Wattanapanichaporn[1], Wanwisa Jantaradach[1], Krisada Wannatong[2], and Tanet Aroonsrisopon[1,*]

[1]Kasetsart University, 50 Ngam Wong Wan Road, Lat Yao, Chatuchak, Bangkok 10900 Thailand
[2]PTT Research and Technology Institute, 71 Moo 2, Phahonyothin Road, km. 78, Wangnoi, Ayutthaya 13170 Thailand

Abstract

Diesel dual-fuel (DDF) operation is a promising alternative engine operating mode. DDF combustion can achieve lower soot and NO_x emissions compared to conventional diesel engine operations. However, DDF engine operations suffer from high HC (mainly CH_4) emissions and poor engine operating stability, especially under low load conditions. The current study investigated cylinder-to-cylinder variations in the DDF combustion in a four-cylinder turbocharged direct-injection diesel engine. All experiments were performed under steady-state engine conditions at 1800 rpm for a range of diesel injection timings and EGR rates.

Data showed that the diesel injection timing and the EGR played an important role in controlling both cyclic variation and cylinder variation in the cylinder outputs. High %EGR was needed to achieve stable DDF combustion in all cylinders. Several factors could render cylinder-to-cylinder variation in the combustion and the combustion stability in each cylinder including the mixture lambda, the EGR distribution, the thermal stratification in the intake, and the charge inhomogeneities. As the cylinder-to-cylinder variation in the combustion became small, the engine efficiency together with HC and CO emissions can be reduced.

Keywords: Diesel dual fuel, Natural gas, Direct Injection, EGR, Cylinder-to-cylinder variations

1. Introduction

Natural gas (NG) has been recognized as one of the promising alternative fuels for internal combustion engines. With the ability to achieve a high compression, a compression-ignition engine produces a higher efficiency than a spark-ignition engine. These reasons have drawn interest in investigating a premixed NG charge diesel-ignited engine. In such a dual fuel engine, NG can be supplied into the intake system or injected into the cylinder. A small amount of diesel fuel is directly injected into the cylinder to promote the autoignition. When converting a diesel engine to a dual fuel engine, the combustion chamber is normally remained unchanged and so is the compression ratio. In the current study, the term "diesel dual fuel (DDF)" engine is referred to as a premixed-natural-gas diesel-ignited engine [1].

DDF engines are capable of reducing both soot and NO_x to levels considerably lower than those of conventional diesel engines. However, at light load, DDF engines are fed with a very lean air-fuel mixture which is hard to auto-ignite and slow to burn, leading to significant amounts of THC and CO emissions [2, 3]. As a premixed charge autoignition mechanism similar to the HCCI combustion, the DDF combustion is governed by both chemical kinetics and the mixing between air and fuels. The chemically kinetic controlled combustion implies that the combustion is affected by thermodynamic state histories that the air-fuel mixture traverses in the cycle. Also, the composition of the charge mixture is one of the main factors influencing the combustion process.

In HCCI engines, the combustion initiation is dependent of several parameters that are not easily controlled like the temperature and pressure histories in the cylinder. So, in a multi-cylinder engine, achieving the same ignition condition in all the cylinders is a challenge. Factors such as the gas exchange, the compression ratio, the cylinder cooling, the fuel supply, and the inlet air temperature can differ from cylinder to cylinder. These differences cause both combustion phasing and load variations between the cylinders, which in the end affect the engine performance and engine-out emissions [4-9].

2. Experimental Setup

2.1 Test Bed Setup

All experiments were performed at PTT Research and Technology Institute. The latest version of a four-cylinder, VN turbocharged Toyota 2KD-FTV common-rail diesel engine was used in the current research. The engine specifications are shown in Table.1.

Table. 1 Engine specifications

Engine type	2KD-FTV
Number of cylinders	4 cylinders, inline arrangement
Number of valves	16 valves (DOHC)
Manifold	Cross-flow with an intercooler and a VN turbocharger
Fuel system	Common-rail, Direct Injection
Displacement volume	2494 cc
Bore × Stroke	92 mm × 93.8 mm
Connecting rod	158.5 mm
Compression ratio	17.4:1
Exhaust valve open	30° BBDC (+150° after firing TDC)
Exhaust valve closed	0° BTDC (+360° after firing TDC)
Inlet valve open	2° BTDC (+358° after firing TDC)
Inlet valve closed	31° ABDC (–149° after firing TDC)
Firing order	1-3-4-2

As an attempt to improve low-load engine operations, the current study investigated the cylinder-to-cylinder variation in the DDF combustion in a four-

*Corresponding Author: E-mail: tanet.a@ku.ac.th

cylinder turbocharged direct-injection diesel engine. The focus of this work was to investigate cylinder-to-cylinder variations in the cylinder outputs and address some important factors for a range of diesel injection timings and EGR rates under steady-state engine conditions.

Fig. 1 shows a schematic of the experimental setup. The engine was coupled to a DC dynamometer. The air at a room condition was drawn to the intake system. A natural gas injector for each cylinder was connected with a rubber hose and attached to the intake runner of the swirl port at which the total length from the NG injector tip to the inlet valves was approximately 345 mm. Diesel fuel was supplied through a common-rail direct injection system. Cylinder pressure data of 150 consecutive cycles from all cylinders were recorded for combustion data analysis. For each cycle, in-cylinder pressure data were recorded with the crank angle resolution of 0.2°. The coolant temperature was maintained at 85°C. The oil temperature was maintained at 90°C. Four wide-band lambda probes were installed at the spacer attached between the exhaust ports and the exhaust manifold to measure exhaust A/F of each cylinder. Exhaust gas emissions were analyzed by using the Horiba MEXA 7100 DEGR gas analyzer. Data of smoke emissions were not available to present in this paper. Although smoke is one of the major common emissions from conventional diesel engines, it was found in our previous study [1] that acceptable DDF combustion produced much less smoke than conventional diesel combustion.

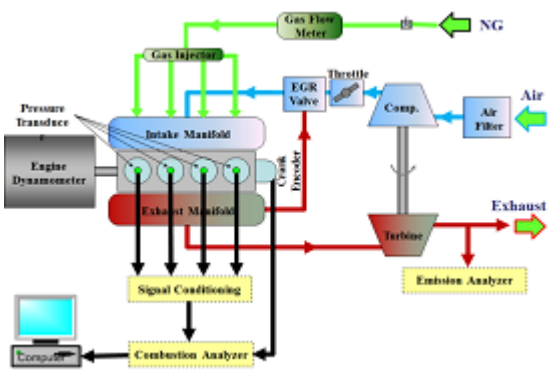

Fig. 1 Schematic of the experiment setup.

2.2 Fuels

Properties of natural gas and diesel fuel in this study are given in Tables 2 and 3.

Table. 2 Properties of natural gas in Thailand (PTT sampling data in 2011)

Methane number	83.0
Higher heating value, MJ/kg	37.71
Lower heating value, MJ/kg	34.10
Stoichiometric A/F	11.68
MW, kg/kmole	22.39
Methane, % by mole	74.2
Ethane, % by mole	5.8
Propane, % by mole	2.3
n-Butane, % by mole	0.4
i-Butane, % by mole	0.5
Larger hydrocarbons (> C_6), % by mole	0.3
CO_2, % by mole	14.5
N_2, % by mole	2.0

Table. 3 Properties of diesel fuel (B3)

Density, kg/m³ (calc.)	0.83
Higher heating value, MJ/kg (calc.)	45.64
Lower heating value, MJ/kg (calc.)	42.75
Stoichiometric A/F (est.)	14.41
MW, kg/kmole (est.)	170
C (est.)	12.30
H (est.)	21.92
O (est.)	0.04

2.3 EGR Calculations

The EGR line was connected from the exhaust runner of the first cylinder (upstream from the exhaust manifold) to the intake line (right after the throttle valve). The EGR flow rate was controlled by adjusting the opening position (EGR set point) of the solenoid valve. The EGR set point could be varied from 0% (fully closed) to 100% (fully opened). One popular technique to estimate the EGR amount is using CO_2 concentrations in the intake manifold and in the exhaust manifold by using Eq. (1) [10]:

$$\%EGR = \frac{[CO_2]_{int}}{[CO_2]_{exh}} \times 100 \quad (1)$$

Notice that as the actual EGR flow rate approaches zero, %EGR calculated by Eq. (1) does not go to zero. To adjust this offset for low EGR cases (say less than 20%), we use the following equation [11]:

$$\%EGR = \frac{[CO_2]_{int} - [CO_2]_{ref}}{[CO_2]_{exh} - [CO_2]_{ref}} \times 100 \quad (2)$$

where $[CO_2]_{ref}$ is the measured CO_2 concentration at the reference point, which is taken as the ambient CO_2 concentration in the laboratory room.

Note that Eq. (1) and Eq. (2) are approxi mations for the EGR molar ratio and should be used with caution. Theoretically, the EGR rate is defined by the ratio between the mass of the EGR and the total mass of the charge mixture entering the cylinder [12]. However, the mass flow rate of EGR was not measured. Using Eq. (1) and Eq. (2) offered a simplified approach to estimate our EGR amount. To allow a better understanding of the characteristics of our engine system, Fig. 2 presents a relation between the EGR set point and the calculated EGR rate (%EGR) at low-load diesel and DDF operations at 1800 rpm. The difference found between diesel and DDF operations was due to the open position of the throttle valve.

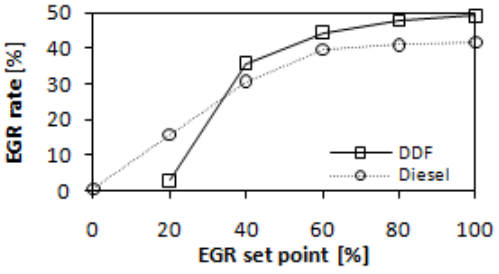

Fig. 2 EGR rates at different EGR set points at low-load diesel and DDF operations at 1800 rpm.

3. Test Matrices

The experiments were divided into 2 matrices with both having the engine speed of 1800 rpm. The first matrix was to observe the DDF combustion characteristics and cylinder output variations as the start of diesel injection (SOI) was varied. In this matrix, the amounts of diesel and natural gas supplied per cycle were kept constant as shown in Table. 4. In the second matrix, we varied the EGR set point to observe combustion characteristics under DDF operations as shown in Table. 5. In this matrix, the throttle was also adjusted to achieve the same air mass flow rate for each EGR set point. Note that for with zero %EGR, we could not achieve stable combustion, thus no data presented.

Table. 4 Engine parameters for the first matrix

Mode	Speed [rpm]	Air [kg/h]	Diesel [kg/h]	NG [kg/h]	Diesel SOI [before TDC]
DDF	1800	57.1	0.63	2.36	45°, 40°, 35°, and 30°

Table. 5 Engine parameters for the second matrix

mode	Speed [rpm]	Air [kg/h]	Diesel [kg/h]	NG [kg/h]	EGR set point [%]
DDF	1800	57.1	0.63	2.36	20%, 40%, 60%, 80%, and 100%

For each data point, the injection signal for each individual fuel injector (for both NG and diesel) was controlled independently to minimize the deviation of injected mass between injectors. The injection timing (in terms of the end of injection) for NG was fixed at 270º bTDC for all DDF runs. For the second matrix, we used a single-pulse diesel signal with the SOI of 38º bTDC.

4. Results and Discussion

This section presents results and discussion of engine performance parameters, pressure data analysis, and engine-out emissions.

4.1 Effects of the Start of Diesel Injection

The DDF operation was investigated using a single-pulse injection signal for all of the test conditions in this work. As the start of injection (SOI) timing was varied from 45º to 30º before TDC (bTDC), the brake torque was increased. Fig. 3 shows torque data and the corresponding engine efficiency for different injection timings.

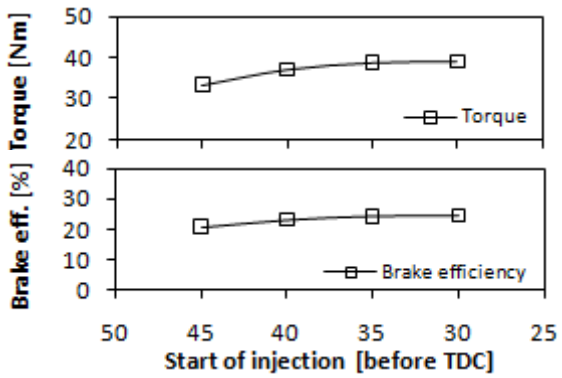

Fig. 3 Brake torque and brake efficiency at different SOI timings.

As the SOI was advanced, the engine torque (also, the efficiency) was reduced. This was due to changes in the combustion in each cylinder. Data of the net IMEP for each cylinder and its cylinder-to-cylinder variation (termed by "IMEPn variation") are shown in Fig. 4. The combustion stability is presented in terms of the cycle-to-cycle variation of the net IMEP recorded over 150 consecutive engine cycles as shown in Fig. 5.

Results showed that the combustion stability in cylinder 1 was least sensitive to the injection timing change compared to other cylinders. This implied that the charge in cylinder 1 could be ignited easier. On the other hand, the combustion stability in cylinder 4 was most sensitive to changes in the injection timing. This also revealed that the charge in cylinder 4 was most difficult to reach autoignition.

Data of the combustion start were recorded and referred to as CA10 as shown in Fig. 6. As the SOI became advanced from 30º to 45º bTDC, the combustion timing was retarded. Regarding data of CA10 (Fig. 6) and IMEPn (Fig. 4) together with its COV (Fig. 5), it appeared that as the onset of combustion shifted later, the combustion stability got worse resulting in a lower cylinder output. At the latest SOI timing, the combustion timings in cylinders 2, 3 and 4 shifted even later from TDC. This corresponded to a significant increase in the COV of IMEPn.

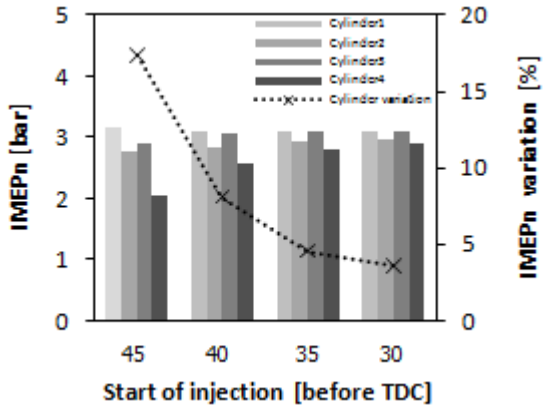

Fig. 4 Net IMEP for each cylinder (clustered bars) and its variation between cylinders (dotted line) for different injection timings.

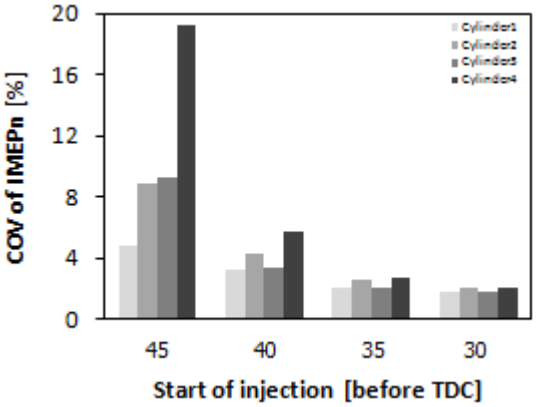

Fig. 5 Coefficient of variation (COV) of the net IMEP for each cylinder at different SOI timings.

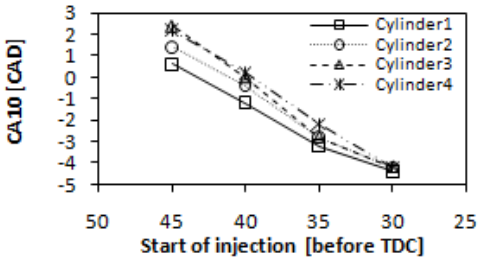

Fig. 6 Start of combustion (CA10) for different SOI timings.

Fig. 7 and 8 compare histories of the cylinder pressure and heat release rates for each cylinder for the injection timings at 45º and 30º bTDC. Notice that the deviations in cylinder pressure and heat release rates between cylinders were more discernible at the SOI of 45º bTDC. For this SOI condition, one could easily observe that cylinder 4 demonstrated the weakest combustion energy release, with cylinder 1 showing the strongest among the four cylinders.

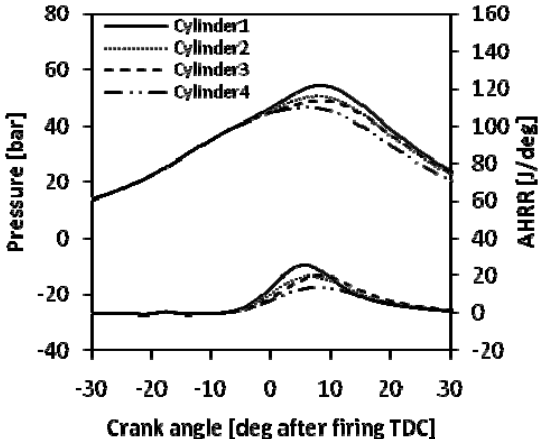

Fig. 7 Pressure and apparent heat release rates with SOI = 45º bTDC.

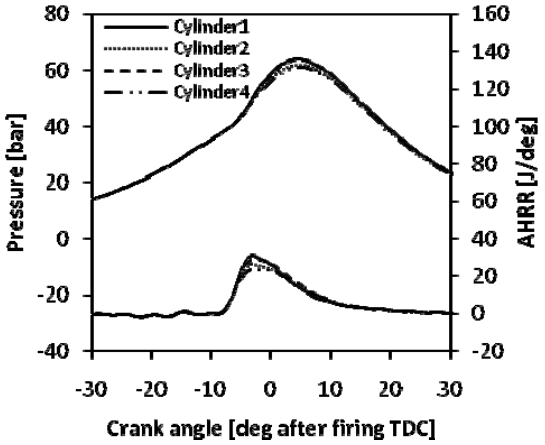

Fig. 8 Pressure and apparent heat release rates with SOI = 30º bTDC.

Based on the discussion in our previous study [13], we found that the cylinder-to-cylinder variation in the combustion was most likely due to the mixture lambda between cylinders. However, we found in the current study that the mixture lambda between cylinders was nearly the same with cylinder 4 having a slightly leaner mixture as shown in Fig. 9. So, in the current study, the mixture lambda would be less pronounced. The dominant factors responsible for the cylinder variations can be the thermodynamic state histories of the local mixture that traverses in the cycle and charge inhomogeneities in each engine cylinder. Note also that with the mixture lambda between cylinders being nearly the same, the charge inhomogeneities, the local charge composition, and its thermodynamic state histories in each cylinder do not need to be identical.

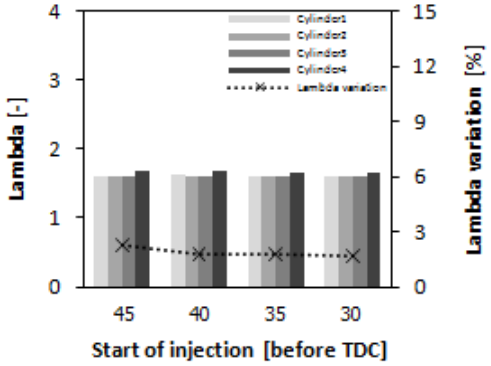

Fig. 9 Measured exhaust lambda (clustered bars) and its variation between cylinders (dotted line) for different injection timings.

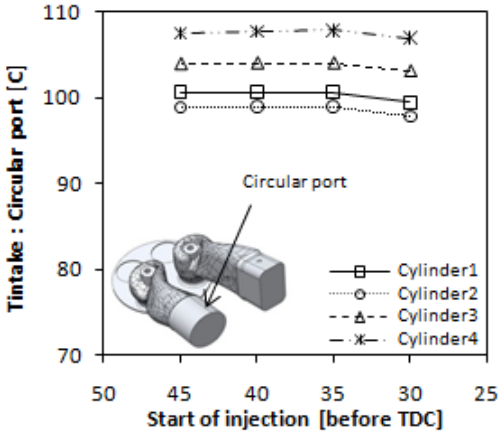

Fig. 10 Intake temperature at the circular port of each cylinder for different injection timings.

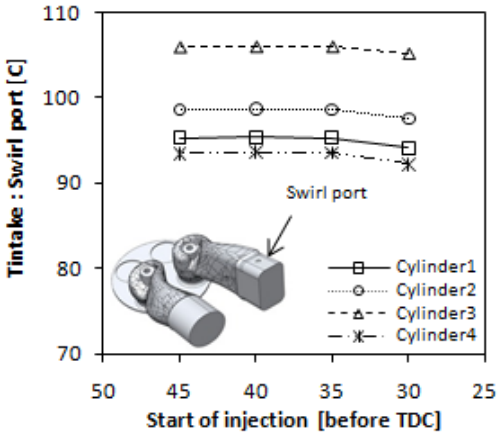

Fig. 11 Intake temperature at the swirl port of each cylinder for different injection timings.

As one possible approach to assess the initial thermodynamic states of the mixture, one can observe data of intake temperatures at the circular port and the swirl port of each cylinder as shown in Fig. 10 and 11. Results showed that the temperature of each cylinder was different. The deviation of port temperatures might be due to the distribution of EGR flow at each intake port being different. As the temperature difference between the two ports became greater, it would promote more thermal stratification in the cylinder charge. The HCCI study by Iverson et al. [14] found that thermal stratification in the intake had a significant impact on the onset of combustion. As such, we proposed that changes in the temperature stratification in the intake mixture can lead to the combustion variations between cylinders in a DDF engine.

Fig. 12 shows data of engine-out emissions. Regarding the emission stand point and the brake engine efficiency (Fig. 3), there appeared an operational window for achieving a low-emission DDF operating condition. We selected the timing of 35º bTDC for the best operation for this test condition. This injection timing operation resulted in only 18 ppm of NO_x, total hydrocarbons (HC, in ppmC) of 7000 ppm, and CO of 0.17%. We prioritized hydrocarbons (especially CH_4) over CO emissions as it would be easier to treat by using an oxidation catalyst compared to CH_4 reduction.

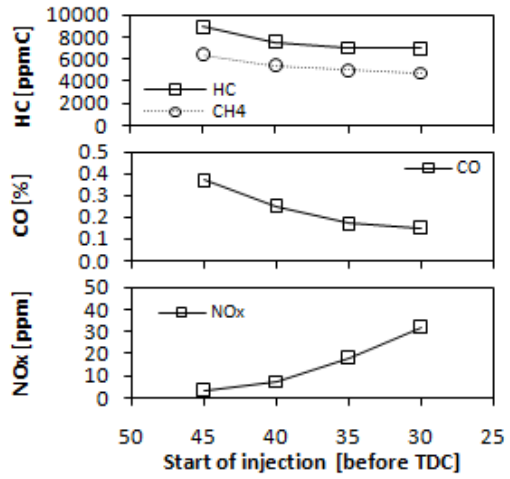

Fig. 12 Hydrocarbons, CO and NO_x engine-out emissions at different SOI timings.

4.2 Effects of EGR

For this data set, we started our preliminary investigation in conventional diesel operation without EGR to reduce the complicity of the operating parameters. Fig. 13 shows diesel mass flow and exhaust lambda of each cylinder with the EGR valve being fully closed. One can see that the diesel supplied to each cylinder was approximately the same, but the measured lambda was varied from cylinder to cylinder. These data suggested that our engine had some variation in the air trapped in each cylinder after IVC.

From the observation above, we now turn our focus to DDF operations. Fig. 14 shows data of brake torque and intake manifold pressure for different %EGR set points. As the EGR rate was reduce, the intake manifold pressure dropped. This caused the pumping work to reduce which then penalized the engine torque. Data of the corresponding efficiency is shown in Fig. 15.

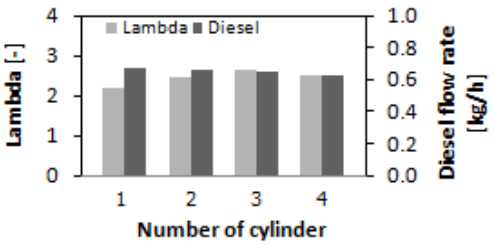

Fig. 13 Lambda and diesel mass flow of each cylinder when the EGR valve is fully closed (zero %EGR) under diesel operation.

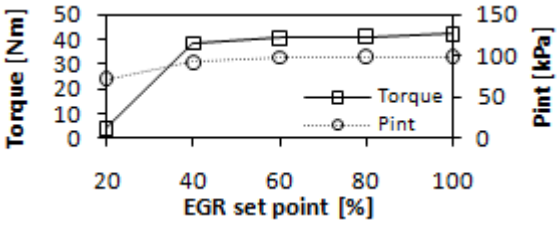

Fig. 14 Brake torque and intake pressure for different EGR set points.

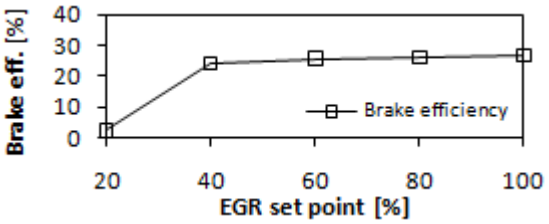

Fig. 15 Brake efficiency for different EGR set points.

Data of the net IMEP and its cylinder-to-cylinder variation are shown in Fig. 16. It appeared a similar trend as found in the previous test matrix that cylinder 1 produced greatest IMEP and cylinder 4 produced the smallest. Furthermore, cylinder 4 had the poorest combustion stability (represented by the cyclic variation of IMEP in Fig. 17). Note that with the 20% EGR set point, we could achieve DDF combustion in only some engine cycles. This resulted in very high COV (also, a drop in the net IMEP) in all cylinders.

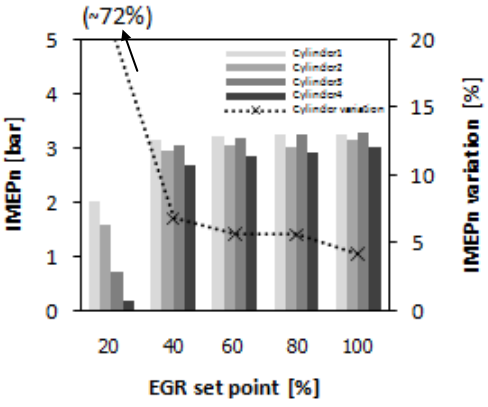

Fig. 16 Net IMEP for each cylinder (clustered bars) and its variation between cylinders (dotted line) for different %EGR set points.

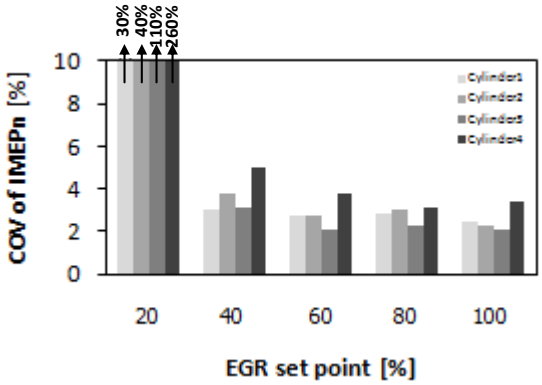

Fig. 17 Coefficient of variation (COV) in net IMEP for different %EGR set points.

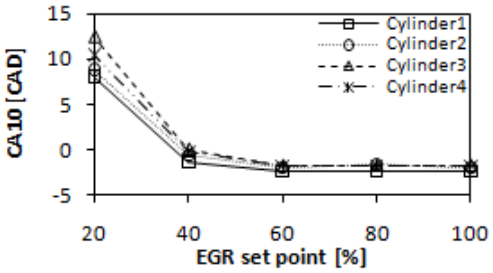

Fig. 18 Start of combustion (CA10) for different %EGR set points.

Fig. 18 shows the start of combustion (in terms of CA10) for different %EGR set points. As the EGR was reduced, the combustion timing was retarded. Fig. 19 and 20 emphasize these changes found with the cylinder pressure and heat release rates for the two extreme cases: 20% and 100% EGR set points. By comparing with data in Fig. 2, the 20% EGR set point corresponded to a nearly zero %EGR rate and the 100% EGR set point (i.e. fully open) had approximately 50% EGR rate.

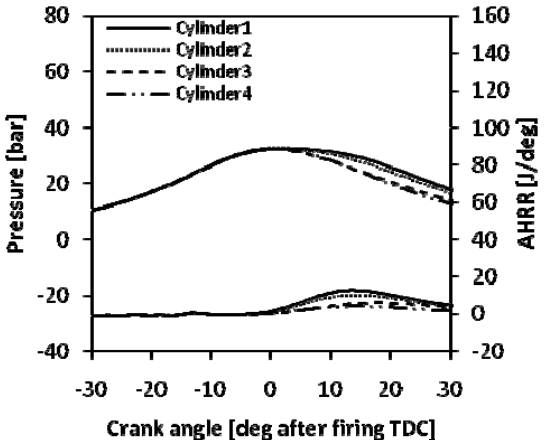

Fig. 19 Pressure and apparent heat release rates for the EGR set point = 20%.

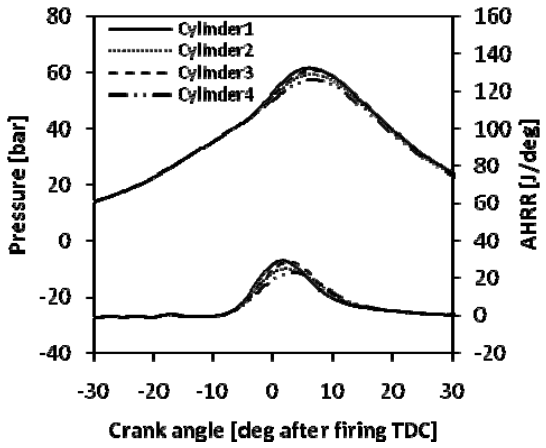

Fig. 20 Pressure and apparent heat release rates for the EGR set point = 100%.

Data of the measured exhaust lambda at each cylinder exit are shown with its cylinder variation in Fig. 21. It was found that the overall lambda was slightly reduced with greater %EGR. Cylinder 4 appeared to have leaner mixture compared to other cylinders for all EGR conditions, especially at lower %EGR. The leaner mixture is more difficult to reach autoignition and produces weaker energy release during the combustion. This is in agreement with the smallest IMEP and the most retarded combustion timing found in cylinder 4.

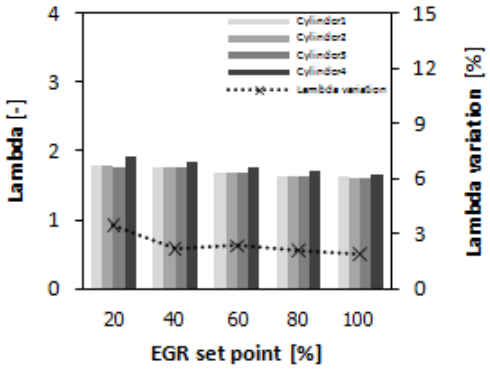

Fig. 21 Measured exhaust lambda (clustered bars) and its variation between cylinders (dotted line) for different %EGR set points.

Data of intake temperatures at the circular port and the swirl port of each cylinder are shown in Fig. 22 and 23. As one would expect, the intake temperature was increased with %EGR. With 20% EGR set point, the deviation of these port temperatures was minimal. As the EGR rate was increased, the discrepancies in port temperatures became larger. This suggested that, not only the variation in the air trapped in each cylinder, but there would be also some variation in the EGR flow into each port and each cylinder. At 100% EGR set point, cylinder 4 had the greatest temperature difference between the two ports which was approximately 16ºC. Therefore, the thermal stratification in the intake would be most pronounced in this cylinder.

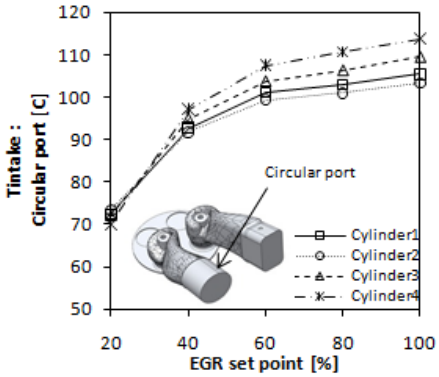

Fig. 22 Intake temperature at the circular port for different %EGR set points.

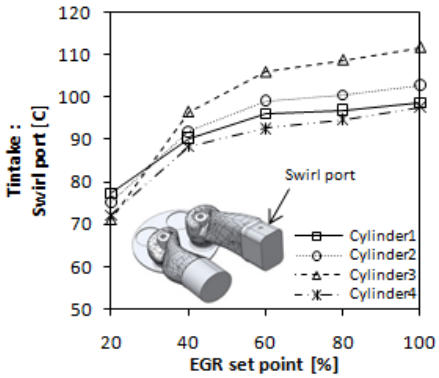

Fig. 23 Intake temperature at the swirl port for different %EGR set points.

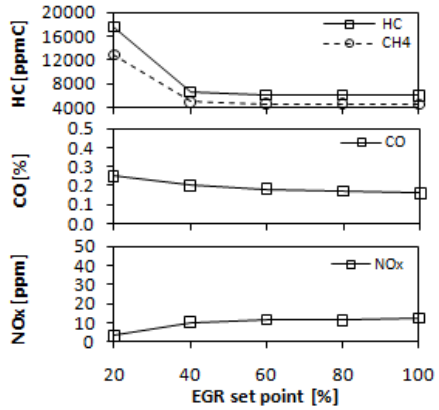

Fig. 24 Effects of EGR on hydrocarbon, CO and NO_x emissions for DDF operations.

It should be noted that the cylinder-to-cylinder variation in the IMEP of diesel dual fuel operations can involve several factors such as the air trapped, the variation of EGR ratio in each cylinder, the thermal stratification in the intake, the deviation in the diesel mass between injectors, the variation in NG trapped in each cylinder, the variation in the residual gas fraction, the turbulent mixing effect on the mixture inhomogeneities, and so on. Further investigation will be required to quantify each of these factors.

Fig. 24 shows engine-out emissions for DDF operations. It was found that hydrocarbon and CO emissions were reduced with greater %EGR. NO_x were very low and slightly increased with %EGR as each cylinder had higher combustion temperatures. One can see that as the cylinder variation and the cyclic variation in the combustion was reduced, reductions in hydrocarbon and CO emissions could be achieved. As such, regulating high EGR was required to obtain good DDF combustion characteristics.

5. Conclusions

Data have been presented for DDF operations in a four-cylinder turbocharged, direct-injection engine. Experiments were conducted under low-load, steady-state operations at 1800 rpm for a range of diesel injection timings and EGR rates. The important findings are summarized as follows:

- The diesel injection timing and the EGR played an important role in controlling both cyclic variation and cylinder variation in the cylinder outputs.
- There could be several factors rendering cylinder-to-cylinder variation in the combustion and the combustion stability in each cylinder including the mixture lambda, the EGR distribution, the thermal stratification in the intake, and the charge inhomogeneities.
- EGR was the important factor responsible for the thermal stratification in the intake.
- High %EGR was required to achieve stable DDF combustion in all cylinders.
- If the cylinder-to-cylinder variation in the combustion is kept minimal, the engine efficiency together with HC and CO emissions can be reduced.

6. Acknowledgement

The authors are sincerely thankful to PTT Public Company Limited for their financial supports throughout the course of this work.

7. References

[1] Tepimonrat, T., Kamsinla, K., Wirojsakunchai, E., Aroonsrisopon, T. and Wannatong, K. (2011). Use of Exhaust Valve Timing Advance for High Natural Gas Utilization in Low-Load Diesel Dual Fuel Operation, SAE Technical Paper 2011-01-1767.

[2] Karim, G. A. (2003). Combustion in Gas Fueled Compression: Ignition Engines of the Dual Fuel Type, *Engineering for Gas Turbines and Power*, vol. 125, July 2003, pp. 827 – 836.

[3] Daisho, Y., Yaeo, T., Koseki, T., Saito, T., Kihara, R. and Quiros, E (1995). Combustion and Exhaust Emissions in a Direct - Injection Diesel Engine Dual-Fueled with Natural Gas, SAE Technical Paper 950465.

[4] HyvÖnen, J., Haraldsson, G. and Johansson, B. (2004). Balancing Cylinder-to-Cylinder Variations in a Multi-Cylinder VCR-HCCI Engine, SAE Technical Paper 2004-01-1897.

[5] Johansson, T., Johanson, B., Tunestål, P. and Aulin, H. (2009). HCCI Operating Range in a Turbo-charged Multi Cylinder Engine with VVT and Spray-Guided DI, SAE Technical Paper 2009-01-0494.

[6] Johansson, T., Johanson, B., Tunestål, P. and Aulin, H. (2009). The Effect to Intake Temperature in a Turbocharged Multi Cylinder Engine operating in HCCI mode, SAE Technical Paper 2009-24-0060.

[7] Ohtsubo, H., Yamauchi, K., Nakazono, T., Yamane, K. and Kawasaki, K. (2007). Influence of Compression Ratio on Performance and Variations in Each Cylinder of Multi-

Cylinder Natural Gas Engine with PCCI Combustion, SAE Technical Paper 2007-01-1877.
[8] Johansson, B. and Einewall, P. (2000). Cylinder to Cylinder and Cycle to Cycle Variations in a Six Cylinder Lean Burn Natural Gas Engine, SAE Technical Paper 2000-01-1941.
[9] Hyvonen, J., Haraldsson, G. and Johansson, B. (2003). Operating Range in a Multi Cylinder HCCI Engine Using Variable Compression Ratio, SAE Technical Paper 2003-01-1829.
[10] Saanum, I., Bysveen, M., Tunestål, P., and Johansson, B. (2007). Lean Burn Versus Stoichiometric Operation with EGR and 3-Way Catalyst of an Engine Fueled with Natural Gas and Hydrogen Enriched Natural Gas, SAE Technical Paper 2007-01-0015.
[11] Aroonsrisopon, T., and Wannatong, K. (2008). Effects of EGR on Diesel Engine-Operating Characteristics under Different Engine Conditions, The 22nd Conference of Mechanical Engineering Network of Thailand (ME-NETT 22), AEC012.
[12] Heywood, J.B. (1988). Internal Combustion Engine Fundamentals, McGraw-Hill, Inc., ISBN 0-07-028637-X.
[13] Jantaradach, W., Wattanapanichaporn, O., Wannatong, K., and Aroonsrisopon, T. (2012) An Investigation into a Sequential Port-Injection of Natural Gas in a Multi-Cylinder Turbocharged Diesel Dual Fuel Engine, The 26th Conference of the Mechanical Engineering Network of Thailand (ME-NETT 26), AEC 2026.
[14] Iverson, R.J., Herold, R.E., Augusta, R., Foster, D.E., Ghandhi, J.B., Eng, J.A., and Najt, P.M. (2005), The Effects of Intake Charge Preheating in a Gasoline-Fueled HCCI Engine, SAE paper 2005-01-3742.

8. Definitions, Acronyms, and Abbreviations

A/F	Air-fuel ratio
bTDC	before firing TDC
CO	Carbon monoxide
CO_2	Carbon dioxide
DDF	Diesel Dual Fuel
EGR	Exhaust gas recirculation
EOI	End of injection
HC	Hydrocarbons
HCCI	Homogeneous Charge Compression Ignition
IMEP	Indicated mean effective pressure
LHV	Low heating value
NG	Natural gas
NO_x	Oxides of nitrogen
SOC	Start of combustion
SOI	Start of injection
TDC	Top dead center
THC	Total hydrocarbons
VN	Variable nozzle (for the turbine)